

1 **Unmixing and mapping components of Northern Ireland's** 2 **geochemical composition using FastICA and random forests**

3
4 Charlie Kirkwood ^{a,*}, Mark Cooper ^b, Antonio Ferreira ^a, David Beamish ^a

5 ^a *British Geological Survey, Environmental Science Centre, Keyworth, Nottingham, NG12 5GG, UK*

6 ^b *Geological Survey of Northern Ireland, Dundonald House, Upper Newtownards Rd, Belfast, BT4 3SB, UK*

7 * Corresponding author. Tel.: +44 1159363344

8 *Email address: cwk@bgs.ac.uk (C.W.Kirkwood)*

9 **Abstract**

10 There is an increasing trend for the collection of multi-sensory quantitative data to support the
11 mapping of geology and environment. In the United Kingdom and Ireland this trend has been led by
12 the Tellus mapping programmes; large scale multidisciplinary surveys which have collected
13 quantitative data by a combination of geophysical survey from the air and geochemical survey on
14 the ground. Such datasets contain a huge amount of geological and environmental information.
15 However, these datasets have tended to be analysed on a variable--by--variable basis rather than as
16 an integrated representation of a single geoenvironmental system. Using the example of Northern
17 Ireland, this paper presents a demonstration of the quality of information that can be extracted
18 through an integrated approach using modern data analytics. Two tools are used: FastICA
19 independent component analysis to unmix the full composition of Northern Ireland's soil
20 geochemistry into meaningful components, and the random forest machine learning algorithm to
21 map these components in high-resolution according to their relationships with geophysical
22 parameters.

23
24 We find that when unmixed to eight independent components, each explaining different aspects of
25 geological and surficial processes, the geochemical features of Northern Ireland can be interpreted
26 concisely. High resolution mapping aids this interpretation, with the random forest approach
27 providing more accurate maps than traditional IDW interpolation for all but one of the components.
28 In addition, by recombining the high resolution maps of independent components into a ternary
29 colour image, a highly detailed output is produced in which all the features of the region's traditional
30 geological map (and more) can be seen, all as a continuous and accurate fully quantitative
31 representation of Northern Ireland's geochemical composition.

32
33
34
35
36
37 *Keywords:*

38 Compositional data analysis

39 Independent component analysis

40 Machine learning

41 Geology

42 Geophysics

43 Tellus Northern Ireland

44 **1. Introduction**

45 Surficial geochemical data contains a wealth of geo-environmental information (e.g. Darnley, 1990;
46 Grunsky et al., 2009; McKinley et al., 2016) and therefore has the potential to improve our
47 understanding of both underlying geology (e.g. Kirkwood et al., 2016b) and the surface environment
48 (e.g. Filzmoser et al., 2009b). Historic barriers to the full utilisation of soil geochemical data have
49 included its relative complexity (high dimensionality and compositional nature; Pawlowsky-Glahn
50 and Egozcue, 2006) and the typically coarse spatial sampling density, which when mapped by
51 traditional spatial interpolation lacks resolution, therefore limiting useful interpretation.

52 Developments in the field of compositional data analysis (CoDA) have provided a set of
53 transformations (Aitchison, 1986; Egozcue et al., 2003) to allow classical dimension reduction
54 techniques such as principal component analysis, factor analysis, and independent component
55 analysis to be non-spuriously applied to compositional data, allowing useful unbiased information
56 to be extracted from bulk geochemical data in the form of compositional components (Filzmoser et
57 al., 2009a; Filzmoser et al., 2009b; McKinley et al., 2016).

58 Meanwhile, developments in the field of machine learning (and the increasing acceptance of
59 geoscientists towards them; e.g. Cracknell et al., 2014; Cracknell and Reading, 2014; Carranza and
60 Laborte, 2015; Harris et al., 2015; Rodriguez-Galiano et al., 2015; Kirkwood et al., 2016a) have
61 provided solutions to the problem of low resolution geochemical maps by modelling geochemistry
62 from high resolution geophysical and remotely sensed data where it is available, with the ability to
63 provide improved prediction accuracy to boot (Kirkwood et al., 2016a).

64 In this paper independent component analysis (FastICA; Hyvarinen, 1999) is applied to the
65 geochemical composition of Northern Ireland's soils after a log-ratio transformation procedure as
66 previously described by Filzmoser et al. (2009a) for compositional principal component analysis. The
67 use of independent component analysis allows the complex mixture of signals within Northern
68 Ireland's soil composition to be unmixed, providing independent and denoised compositional

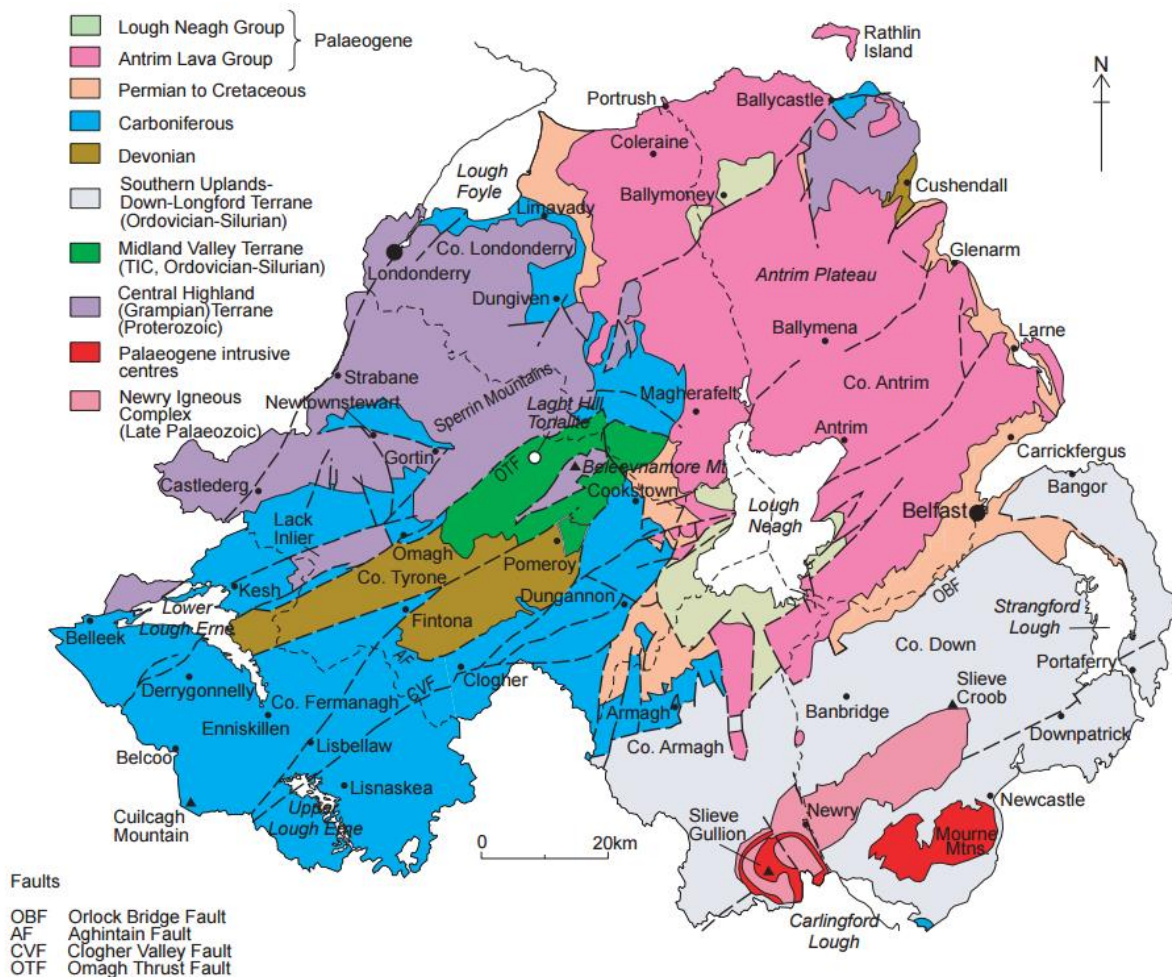
69 components, each representing a 'latent variable' attributable to a particular process. These
70 components are subsequently mapped using the random forest regression tree ensemble approach
71 (Breiman, 2001) supported by high -resolution geophysical survey data to provide maps with greater
72 detail and accuracy than their traditionally interpolated equivalents. The work is presented as a
73 demonstration and visualisation of the quality of information that can be extracted by applying
74 modern methods of data analysis to integrated multi-source survey data.

75 **2. Materials**

76 *2.1 Study area*

77 The study area, Northern Ireland, is a constituent unit of the United Kingdom of Great Britain and
78 Northern Ireland and is situated in the northeast of the island of Ireland. The geology of Northern
79 Ireland can be considered in four main domains (Fig. 1; Cooper, 2004). Firstly, in the north west are
80 the oldest rocks of Northern Ireland; the Proterozoic basement of the Central Highland or Grampian
81 Terrane. Secondly, in the south east are Ordovician-Silurian sedimentary rocks of the Southern
82 Uplands-Down-Longford Terrane, intruded by Late Caledonian and Palaeogene granitoids. Thirdly, in
83 the south west are Devonian-Carboniferous sedimentary rocks, and finally, in the north east, are the
84 Cenozoic (Permian-Cretaceous) rocks that most notably include the early Paleogene Antrim Lava
85 Group. In addition to this impressive and variable bedrock history, Northern Ireland has experienced
86 repeated glaciations during the Quaternary that have resulted in the formation of a range of glacial
87 deposits that mantle the landscape. For some of these deposits their geochemical composition
88 reflects the underlying bedrock source (Dempster et al., 2013), whilst for others there is a disparity
89 because of transport or processes of deposition. Each of these various domains and their
90 constituent lithologies (bedrock and superficial deposits) can be expected to impose a unique
91 geochemical signature on the composition of the soils that overlie them.

92
93

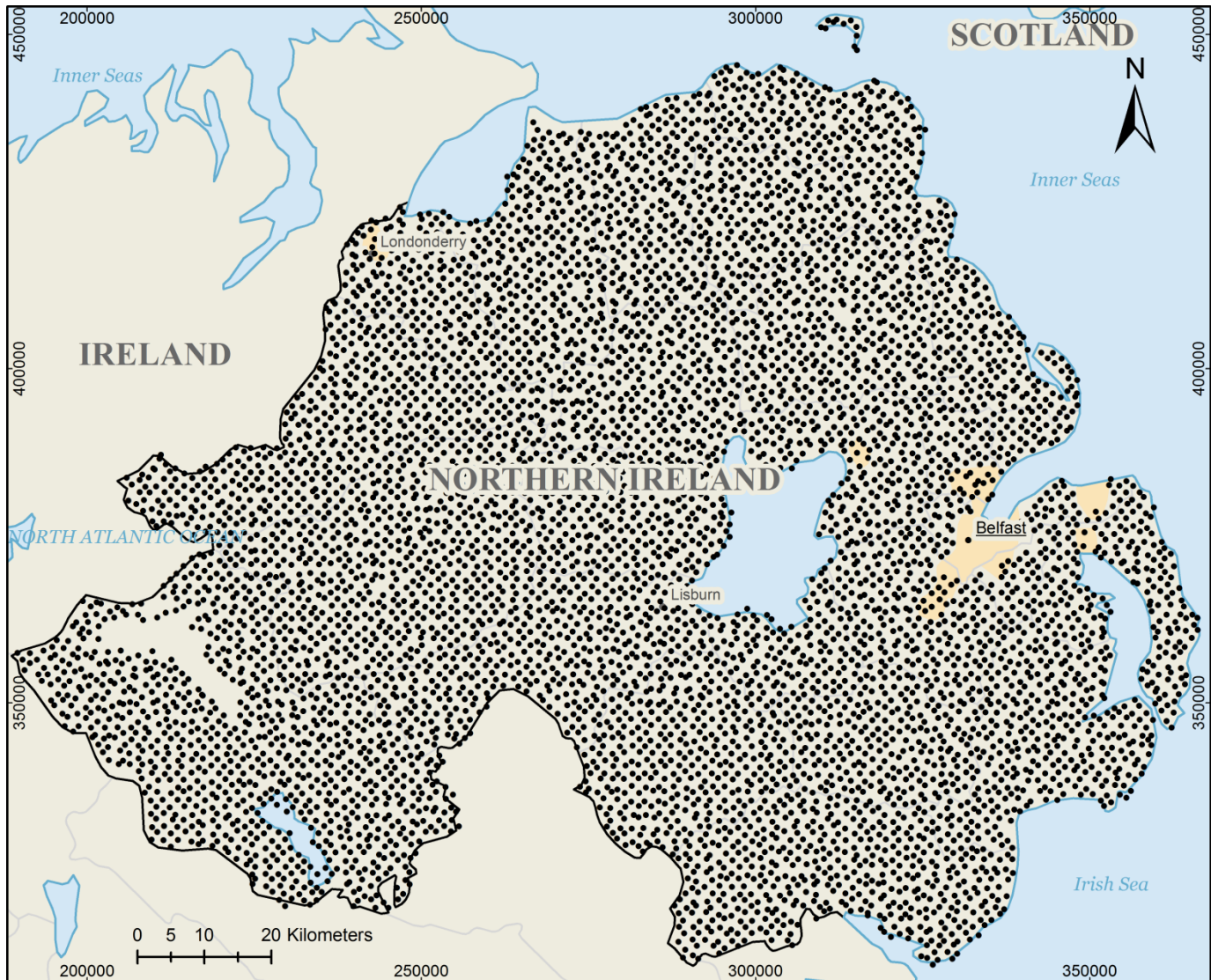


94
95 **Fig. 1.** Simplified bedrock geology of Northern Ireland, from Cooper (2004).
96

97 2.2 Soil geochemical data

98 The soil geochemical data used in this study comes from the analysis of 6862 shallow soil samples
99 (Fig. 2) collected for the Tellus Northern Ireland project between the years of 2004 and 2006 (Young
100 and Donald, 2013). Samples were collected in accordance with standardised methods developed by
101 the British Geological Survey for the Geochemical Baseline Survey of the Environment (G-BASE)
102 project (Johnson et al., 2005). Each sample represents material collected at 5-20cm depth at a
103 randomly positioned locality within each 1km grid square of the Irish National Grid, subject to the
104 avoidance of immediate anthropogenic influence where possible. This study uses the data from XRF
105 analysis, which provided concentration data for the following 52 elements (with major elements as
106 oxides): Ag, Cd, In, Sn, Sb, Te, I, Cs, Ba, La, Ce, Na₂O, MgO, Al₂O₃, SiO₂, P₂O₅, SO₃, K₂O, CaO, TiO₂,

107 MnO, Fe₂O₃, Cl, Sc, V, Cr, Co, Ni, Cu, Zn, Ga, Ge, As, Se, Br, Rb, Sr, Y, Zr, Nb, Mo, Nd, Sm, Yb, Hf, Ta,
108 W, Tl, Pb, Bi, Th, U, and R – the unmeasured remainder of the full composition. The elemental
109 analyses were conducted by the British Geological Survey.



110
111 **Fig. 2.** Locations of 6862 shallow soil samples collected and chemically analysed for the Tellus Northern Ireland project.

112 *2.3 Geophysical data*

113 In addition to providing a comprehensive geochemical survey of the ground, the Tellus Northern
114 Ireland project also flew a high resolution geophysical survey from the air (Beamish and Young,
115 2009; Young and Donald, 2013). The airborne geophysical survey acquired magnetic, radiometric,
116 and frequency-domain electromagnetic data (Hodgson and Young, 2016), and is supplemented in
117 this study by pre-existing elevation and gravity data. Each measured geophysical variable (Table 1)
118 was interpolated to a 100m grid prior to use in this study. Magnetics data was interpolated using a

119 bicubic spline, while all other variables were interpolated using a minimum curvature method, as is
120 common practice for geophysical data (Hinze et al., 2013).

121 **Table 1**

122 Explanations of the geophysical and remotely sensed predictor variables used in the high resolution mapping.

Variable name	Explanation
Elevation	Digital Terrain Model
Regional Bouguer Anomaly	Gravity survey bouguer anomaly
Residual Bouguer Anomaly	Gravity survey high pass filtered bouguer anomaly
MAG_RTP	Total magnetic intensity, reduced to pole
MAG_RTP_HGM	Horizontal gradient of MAG_RTP
MAG_RTP_1VD	1 st vertical derivative of MAG_RTP
MAG_AS	Analytical signal of total magnetic intensity
Radiometrics_uranium	Uranium counts from gamma ray spectrometry
Radiometrics_thorium	Thorium counts from gamma ray spectrometry
Radiometrics_potassium	Potassium counts from gamma ray spectrometry
Radiometrics_total_count	Total count of unmixed gamma ray signal
COND_3K	Ground conductivity – 3Khz band
COND_14K	Ground conductivity – 14Khz band

123 **3. Methods**

124 *3.1 compositional independent component analysis (ICA)*

125 All data analysis and modelling was conducted in R (R Core Team, 2016). In order to extract
126 meaningful components of soil composition from the geochemical data, compositional independent
127 component analysis was used. The kind of geochemical data used in this study should be treated
128 compositionally because the variables (element concentrations) are not truly independent of each
129 other, but are confined to sum to the total of the closed composition, i.e. 100% or 1 000 000 mg/kg
130 (Pawłowsky-Glahn et al., 2007). The variables therefore have an imposed tendency to negatively
131 correlate; as one increases, others must decrease and vice versa. The values of a single variable are
132 therefore entirely dependent on the degree of dilution by other variables. Each variable is therefore
133 said to carry only relative information (Aitchison, 1986): what matters are the ratios between
134 variables rather than their individual values. Applying classical correlation-based statistical methods
135 directly to such data is therefore bound to produce spurious and misleading results (Pearson, 1896;

136 Chayes, 1960). Instead, the data must first be transformed into a more appropriate mathematical
137 space, where correlation measures are replaced with measures of the stability of ratios between
138 variables. The isometric log-ratio- transformation (ilr; Egozcue et al., 2003) provides this, and is the
139 first step of the compositional ICA procedure.

140 ICA was conducted using the FastICA algorithm (Hyvarinen, 1999). ICA was chosen over principal
141 component analysis for its ability to unmix (make orthogonal and independent) trends which are not
142 necessarily orthogonal in the original feature space. It does this by separating components according
143 to the shapes of their distributions (their non-Gaussianity) assuming that they are not perfectly
144 normal distributions but differ in skewness and kurtosis. This makes it more powerful than principal
145 component analysis, which can only rotate the input data to maximise variance along the principal
146 axes, and so may well not align with the true 'latent variables' within the data. As a result of its
147 power, ICA has become a preferred technique for making sense of complex mixtures, for example in
148 neuroscience it is used to unmix electroencephalographic (EEG) data (e.g. Makeig et al., 1996;
149 Delorme and Makeig, 2004) and it has had some recent uptake in geochemical applications (Liu et
150 al., 2014; Yang and Cheng, 2015).

151 The ICA parameters for this study were selected manually with the aim of maximising the
152 orthogonality (independence) of the output components. This was assessed subjectively by viewing
153 output components as pairwise scatter plots. It was found that unmixing to eight components using
154 deflation and an exponential G function (Hyvärinen and Oja, 2000) provided the best results: trends
155 within the output data became most strongly aligned with the component axes, indicating that the
156 ICA algorithm had been successful in unmixing the data into independent components. By applying
157 FastICA to ilr transformed data, the process is unaffected by the spurious correlations within the
158 original closed-composition geochemical data, and can be expected to produce valid and meaningful
159 results (Filzmoser et al., 2009a).

160 A complication of the ilr transformation is that the dimensionality of the data is reduced by one in
161 the process, i.e. in this case 53 concentration variables are transformed into 52 log-ratio variables,
162 losing their names (and their immediate meaning) in the process. To allow interpretable
163 visualisations of element loadings to be made after ICA the results were subsequently transformed
164 from isometric log-ratio-s to centred log-ratios (CLR; Aitchison, 1986). Through CLR transformation,
165 the original number of variables is restored, and each can be referred to by its original name, though
166 in fact as CLRs they represent log-ratios of the original element concentrations against the geometric
167 mean of the whole measured composition.

168 *3.2 Mapping soil compositional components in high resolution*

169 The output soil compositional components were mapped in high resolution using the random forest
170 (Breiman, 2001) algorithm to learn the physio-chemical relationships present between the high
171 resolution geophysical survey data and the coarsely sampled geochemical data. The same technique
172 has provided improved prediction accuracy and insight into the concentrations of the majority of
173 elements in south west England (Kirkwood et al., 2016a), and has been gaining momentum in recent
174 years for predictive mapping applications in general (e.g. Henderson et al., 2005; Gislason et al.,
175 2006; Lawrence et al., 2006; Evans et al., 2011; Wiesmeier et al., 2011; Rodriguez-Galiano et al.,
176 2012; Cracknell et al., 2014; Cracknell and Reading, 2014; Carranza and Laborte, 2015; Harris et al.,
177 2015; Rodriguez-Galiano et al., 2015). In this study the R package 'Rborist' is used (Seligman, 2016),
178 with 1001 trees, and a minimum node size of 1. To assess the accuracy of each map, 10-fold cross
179 validation is used, and metrics are compared to the equivalent map produced by Inverse Distance
180 Weighted (IDW) interpolation, the method that has historically been used to produce geochemical
181 maps in the UK.

182

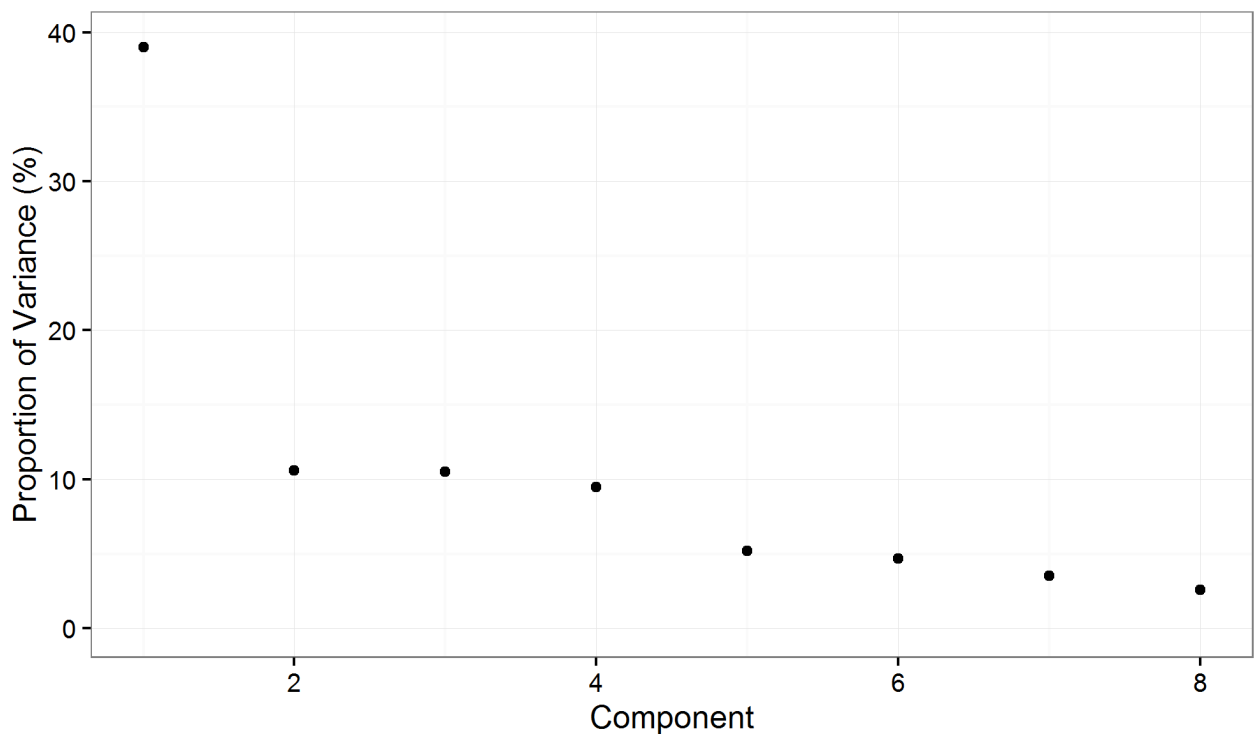
183

184 **4. Results**

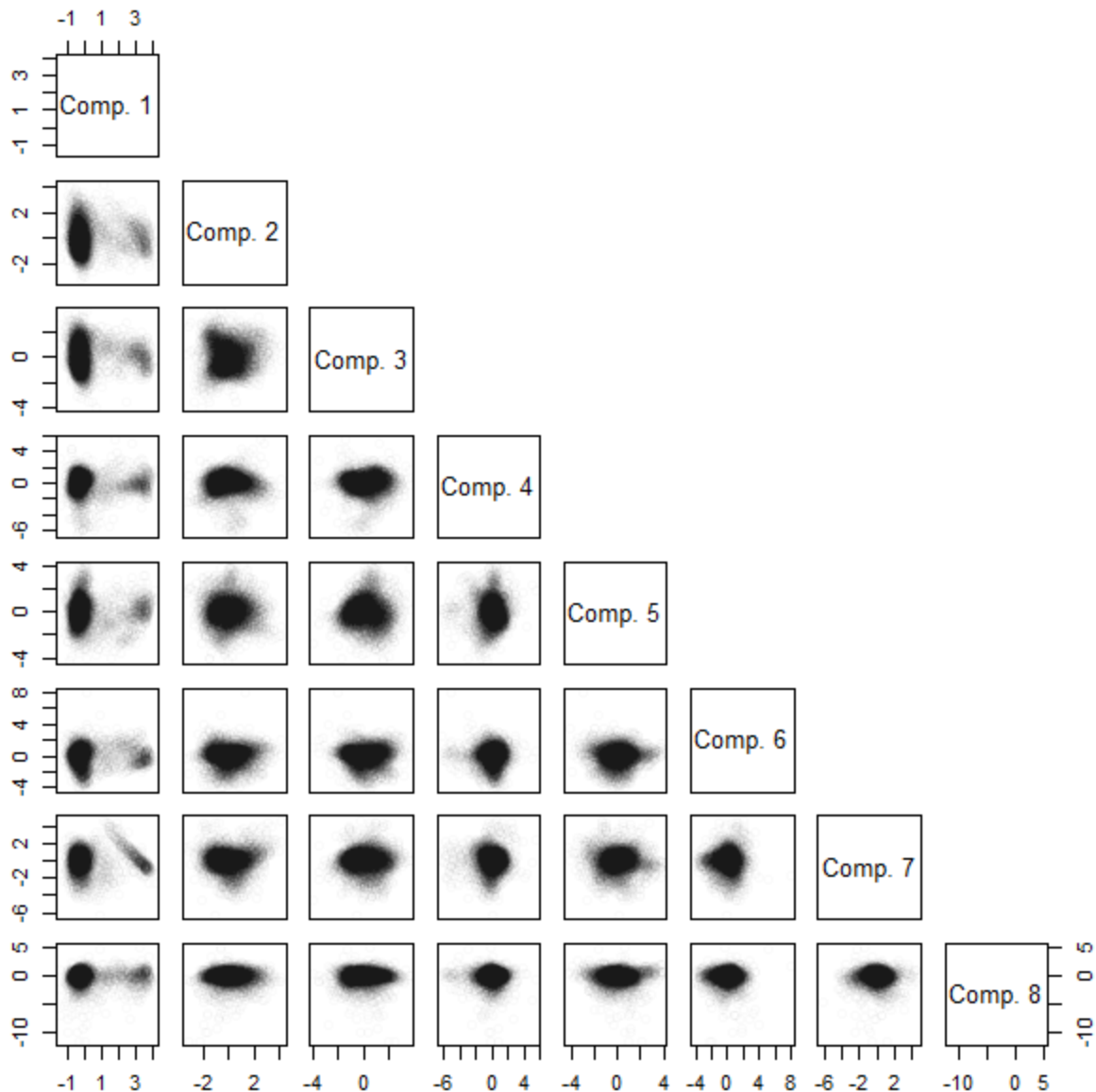
185 *4.1 Compositional ICA overview*

186 The variance explained by each of the eight independent components of the ilr -transformed soil
187 geochemical data (Fig. 3) reveals that 39% of the total variance is explained by the first component
188 alone, with components two, three, and four providing an additional 10.6, 10.5 and 9.5% of
189 explanation respectively. The eight components together explain 86% of the total variance in
190 Northern Ireland's soil composition and are highly independent (Fig. 4). Component eight itself
191 explains just 2.6% of the variance, but can be assumed to have some importance, as the ICA was less
192 successful (outputs appeared increasingly co-dependent) when run with seven components or less.
193 The 14% of variance that is not captured within the eight independent components can be assumed
194 to be unstructured noise, as again the ICA produced correlated outputs when run with more than
195 eight components. The eight independent components used in this study can therefore be taken as a
196 'subjectively optimal' summary of Northern Ireland's soil chemistry, with only minimal loss.

197



198 **Fig. 3.** Proportion of variance explained by each independent compositional component of Northern Ireland's soil
199 geochemical data. The explanations sum to 86%, indicating that 14% of the original variance has been discarded as 'noise'.
200
201



202
 203 **Fig. 4.** Pairwise scatter plots of the eight independent components of Northern Ireland's soil chemistry. The success of the
 204 ICA procedure is evident in the general absence of correlation between components: trends within the point clouds tend to
 205 be aligned with the component axes i.e. either horizontally or vertically, thus indicating their independence.
 206

207 *4.2 Random forest independent component maps, with component loadings*

208 The use of random forests to map the eight independent components of Northern Ireland's soil
 209 chemistry was successful in producing more accurate maps than IDW interpolation for all but one
 210 component (for which the difference is negligible), as evaluated by 10-fold cross-validation (Table 2).

211 In every case, the random forest maps offer a detailed format from which to visualise the
 212 relationships between geochemistry and environment. The component maps have been visualised
 213 using the perceptually uniform Viridis colour scale (Garnier, 2015).

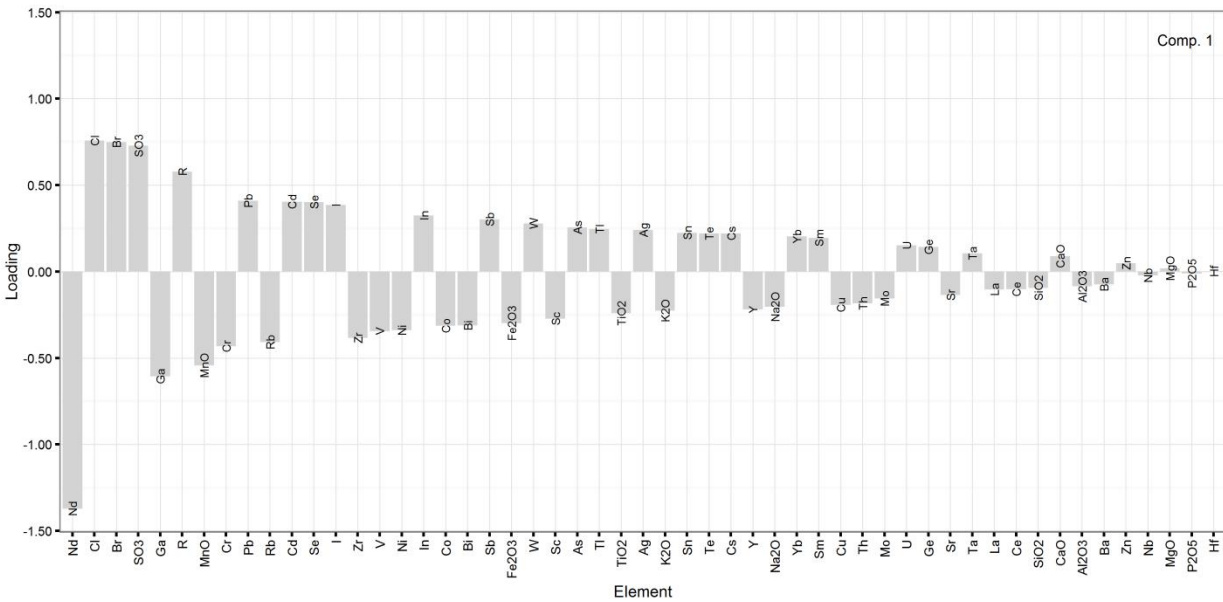
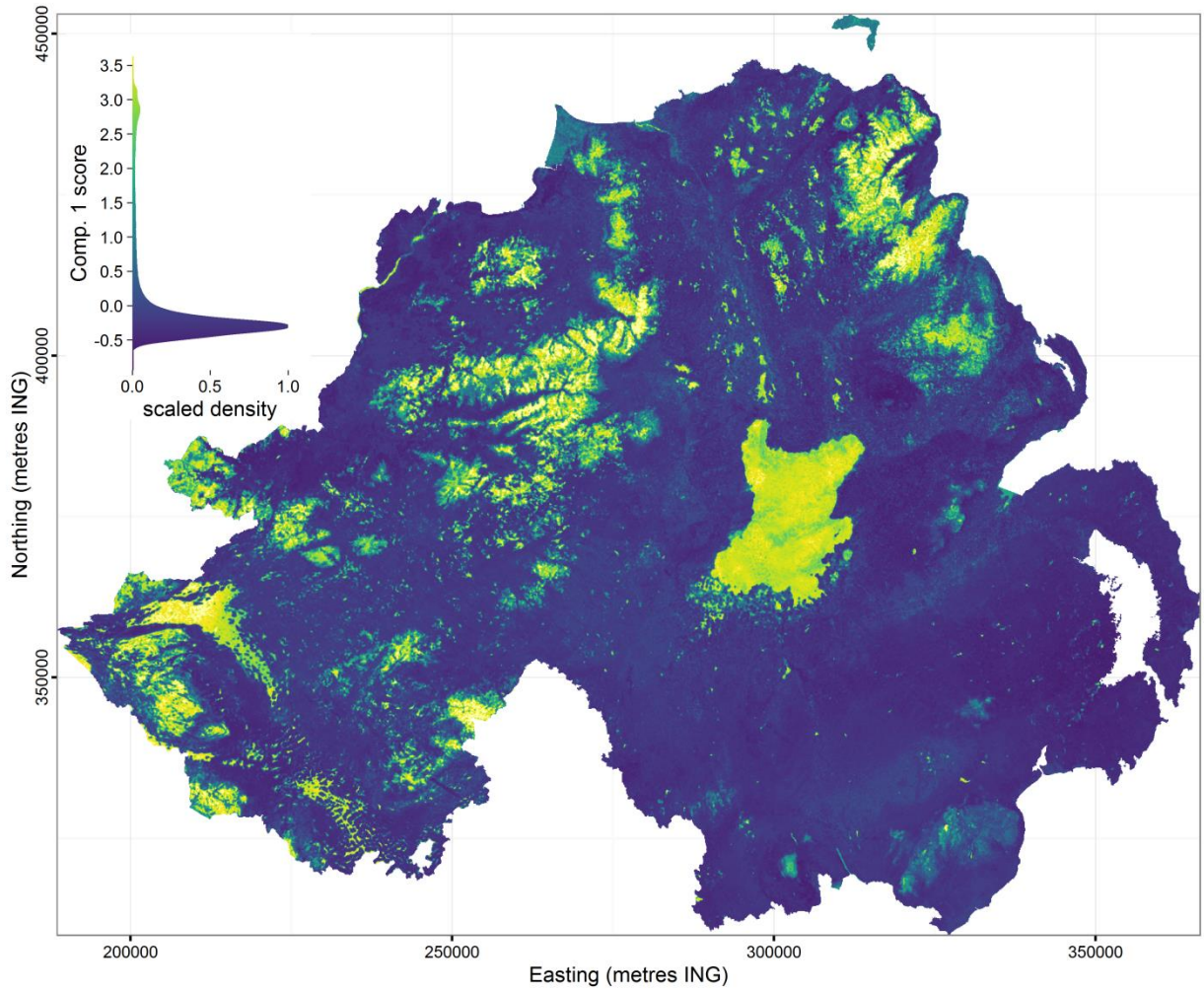
214 **Table 2**

215 Root-mean-square errors (RMSEs) of predictions made by random forest and IDW interpolation in mapping the eight
216 independent components. Lower is better. This error was measured through 10-fold cross-validation.

	Comp. 1	Comp. 2	Comp. 3	Comp. 4	Comp. 5	Comp. 6	Comp. 7	Comp. 8
Random forest	0.60	0.68	0.61	0.59	0.65	0.79	0.88	0.89
IDW interpolation	0.85	0.74	0.70	0.67	0.72	0.78	0.91	0.90

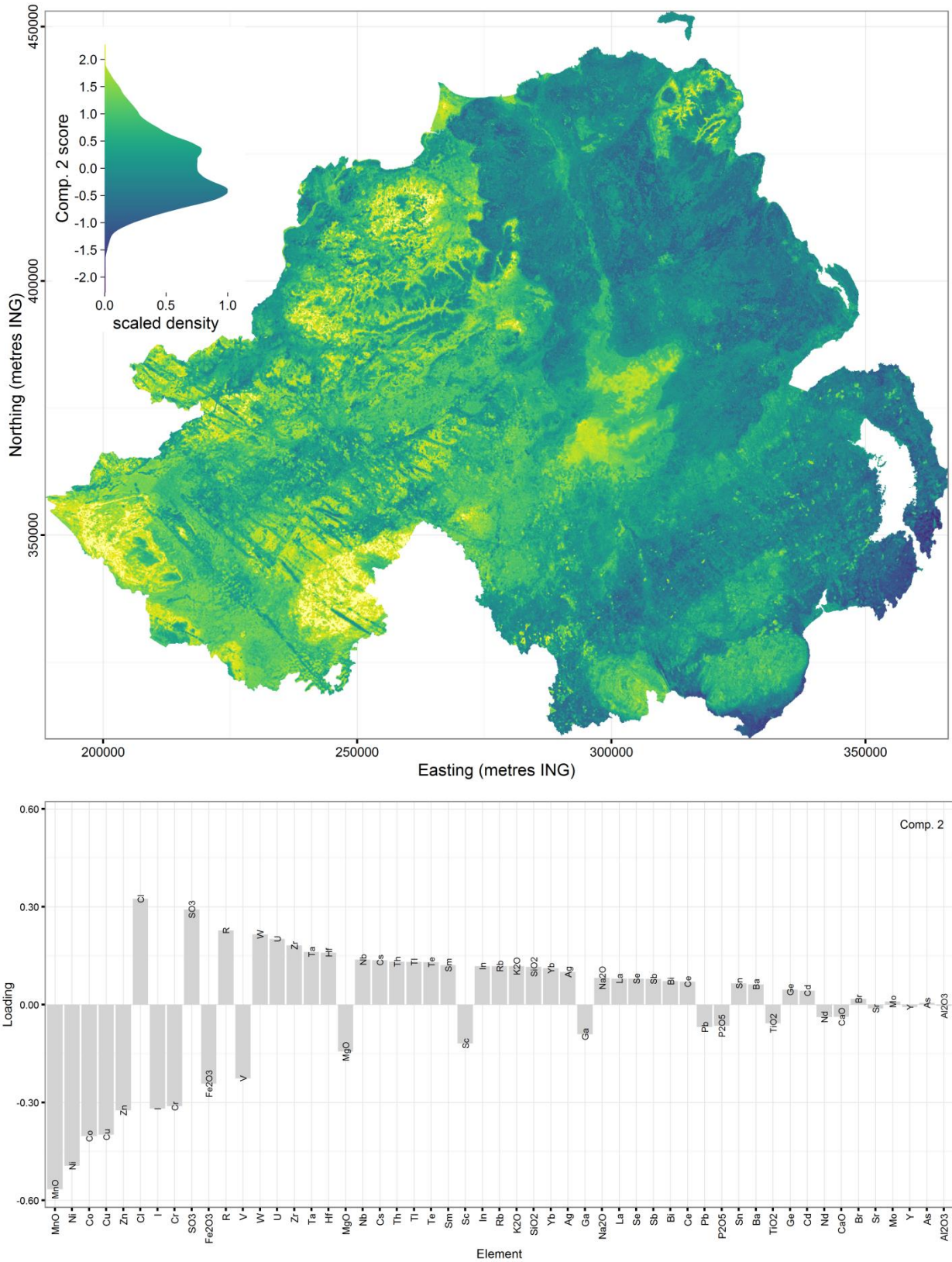
217

218



220
221
222
223

Fig. 5. Top) Map of independent component 1 of ilr transformed shallow soil geochemistry, produced using geophysical covariates and the random forest machine learning algorithm. Bottom) Element loadings on independent component 1, as centred log-ratios (relative enrichments/depletions).



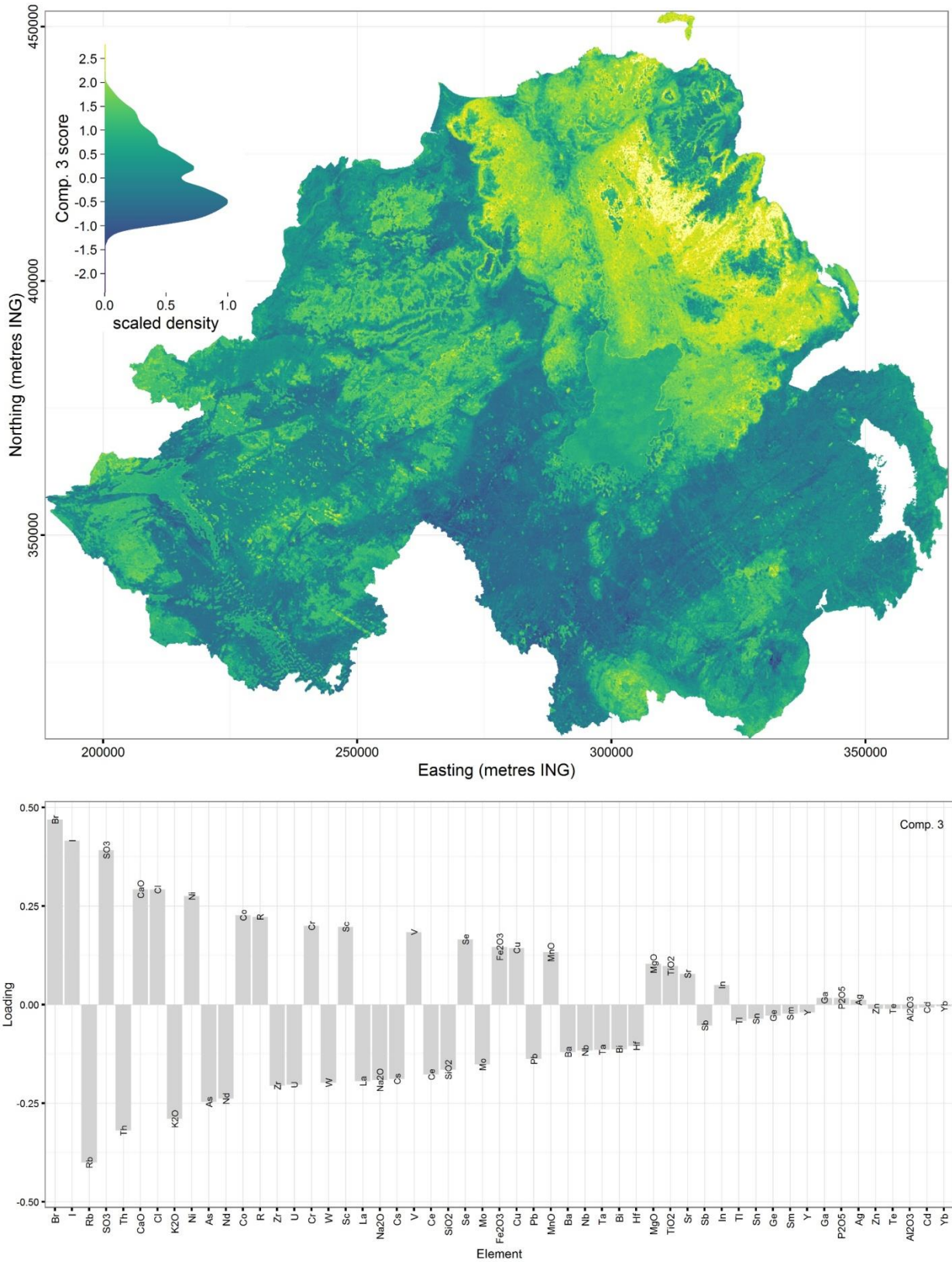
225

226

227

228

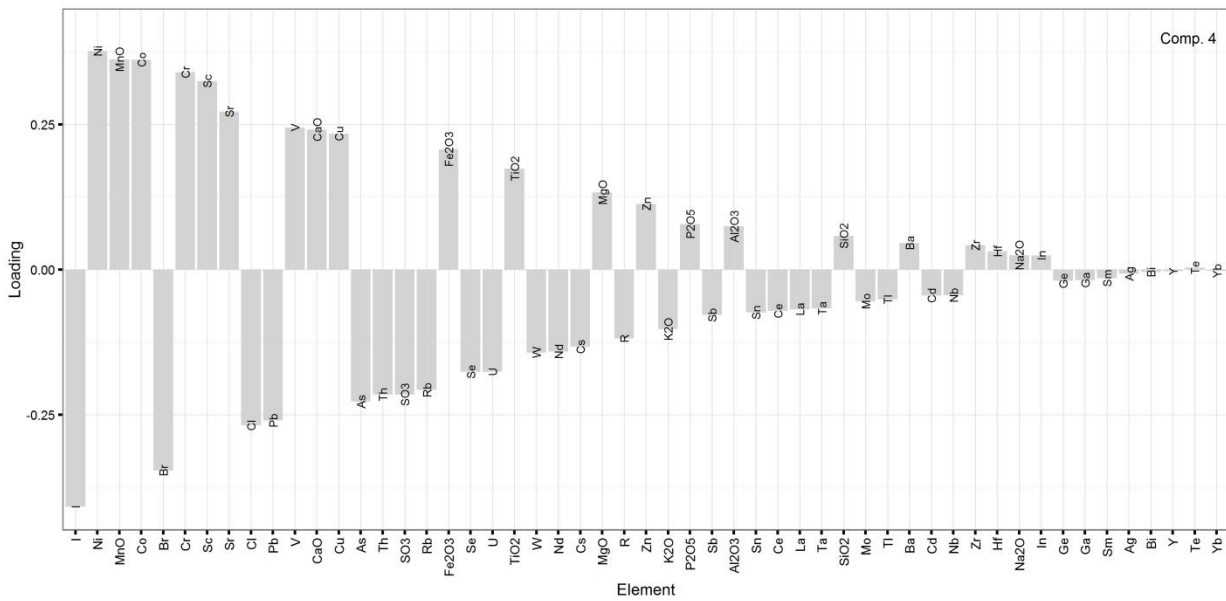
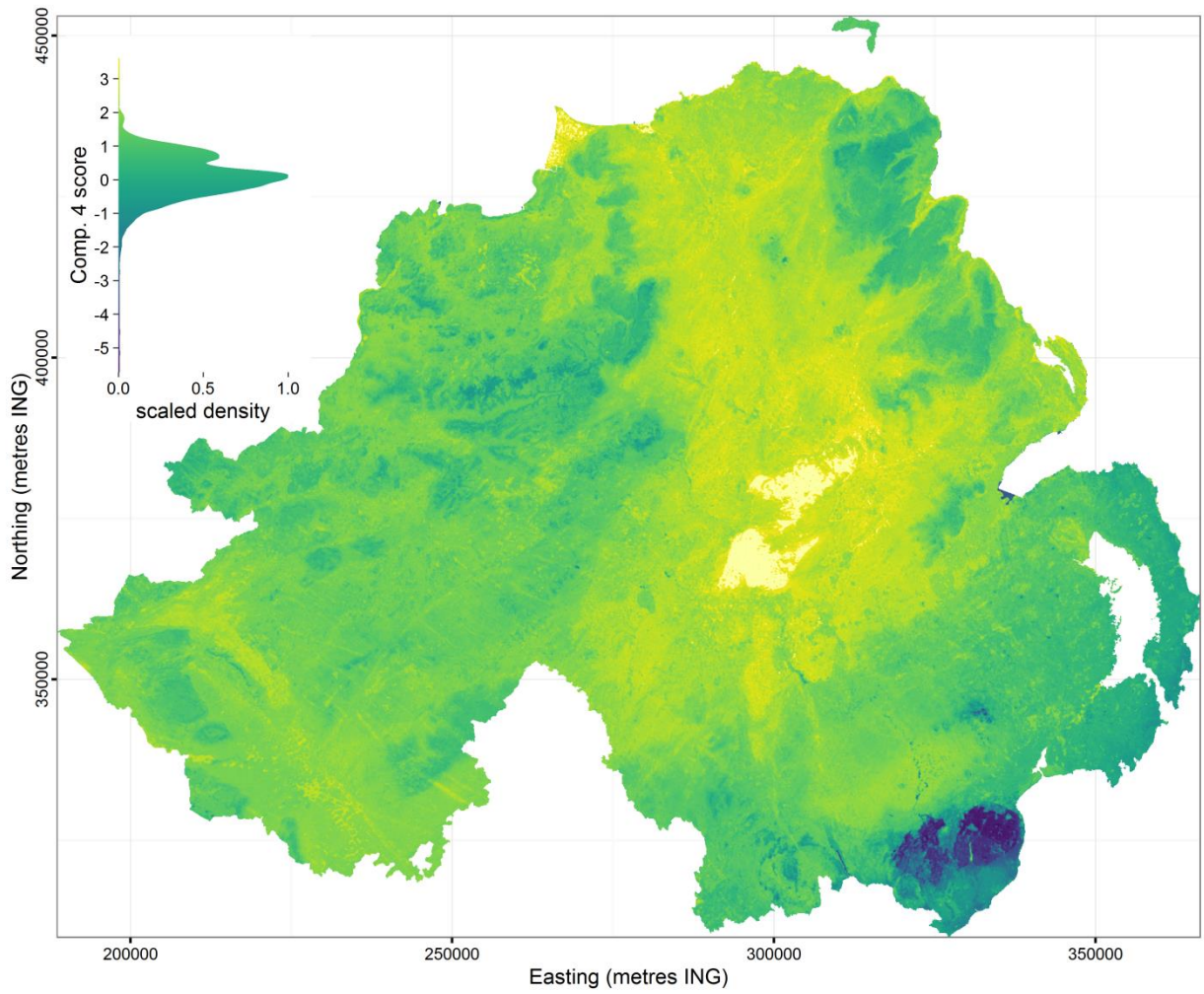
Fig. 6. Top) Map of independent component 2 of 1lr transformed shallow soil geochemistry, produced using geophysical covariates and the random forest machine learning algorithm. Bottom) Element loadings on independent component 2, as centred log-ratios (relative enrichments/depletions).



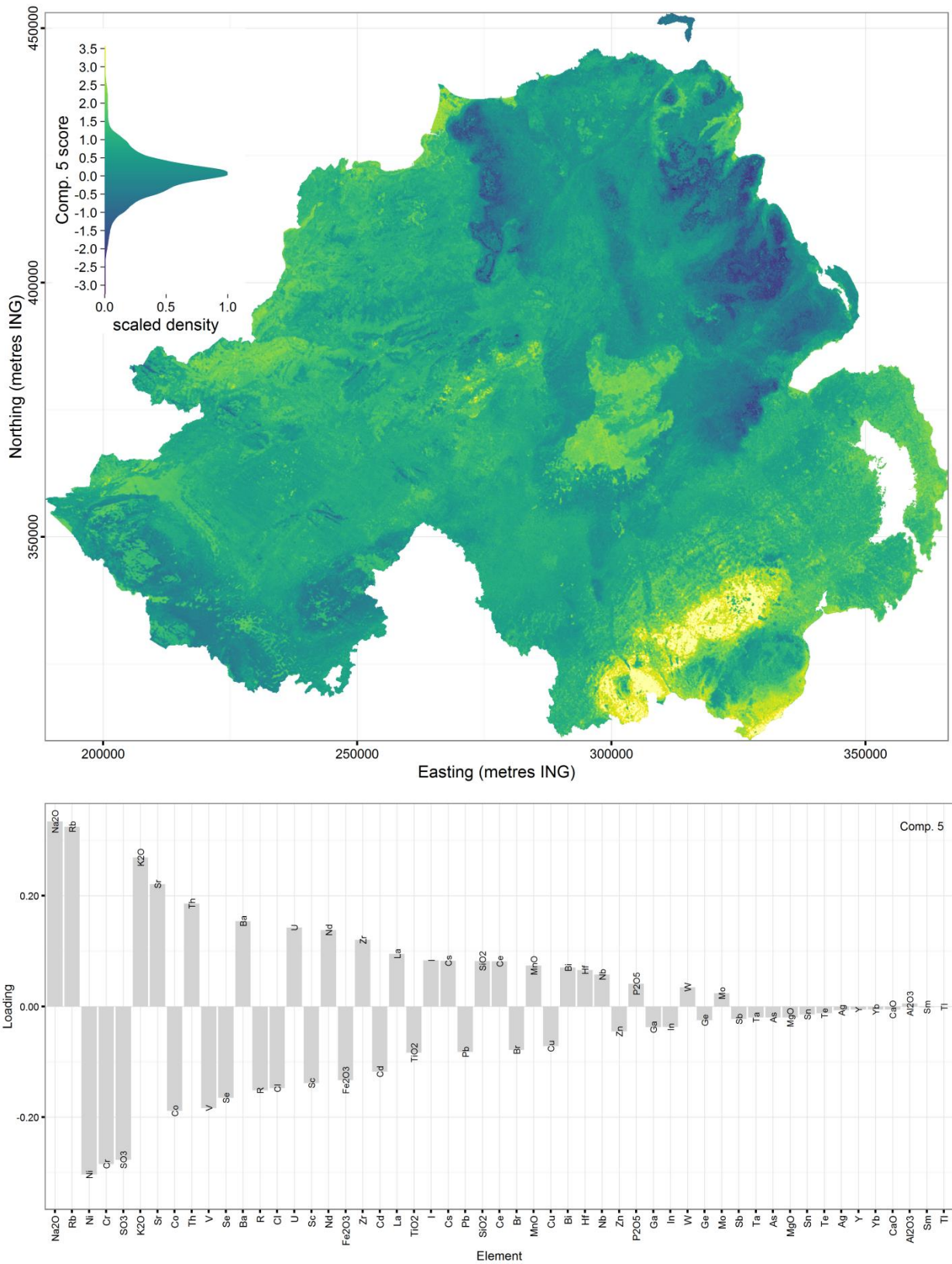
230

231
232
233

Fig. 7. Top) Map of independent component 3 of IIR transformed shallow soil geochemistry, produced using geophysical covariates and the random forest machine learning algorithm. Bottom) Element loadings on independent component 3, as centred log-ratios (relative enrichments/depletions).



236 **Fig. 8.** Top) Map of independent component 4 of irlr transformed shallow soil geochemistry, produced using geophysical
 237 covariates and the random forest machine learning algorithm. Bottom) Element loadings on independent component 4, as
 238 centred log-ratios (relative enrichments/depletions).

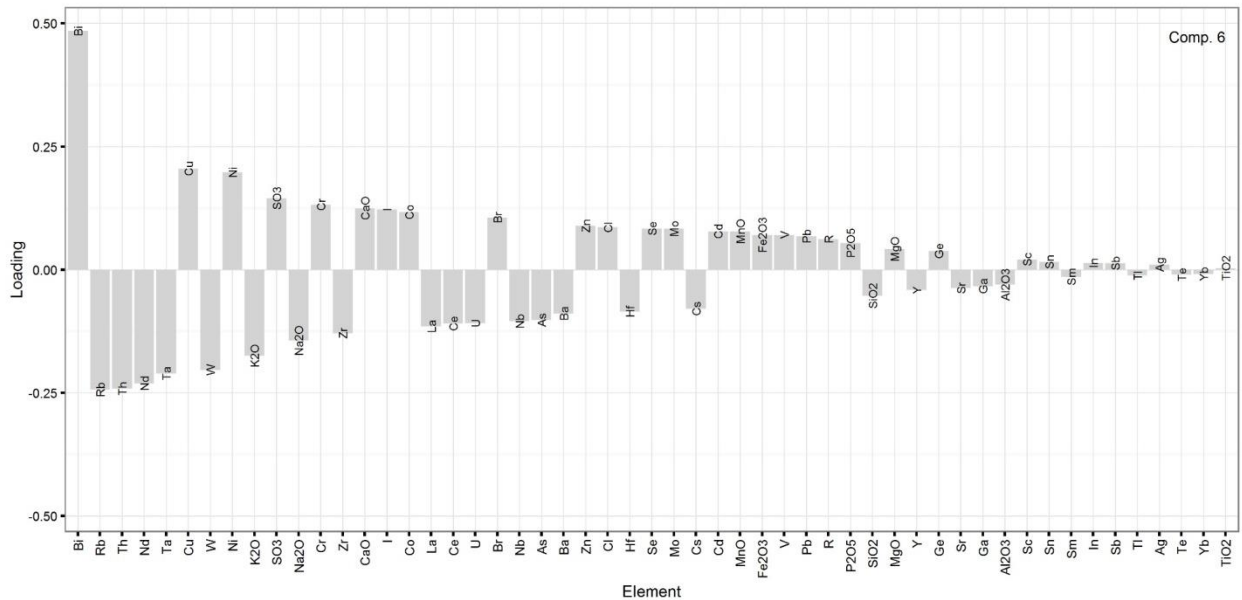
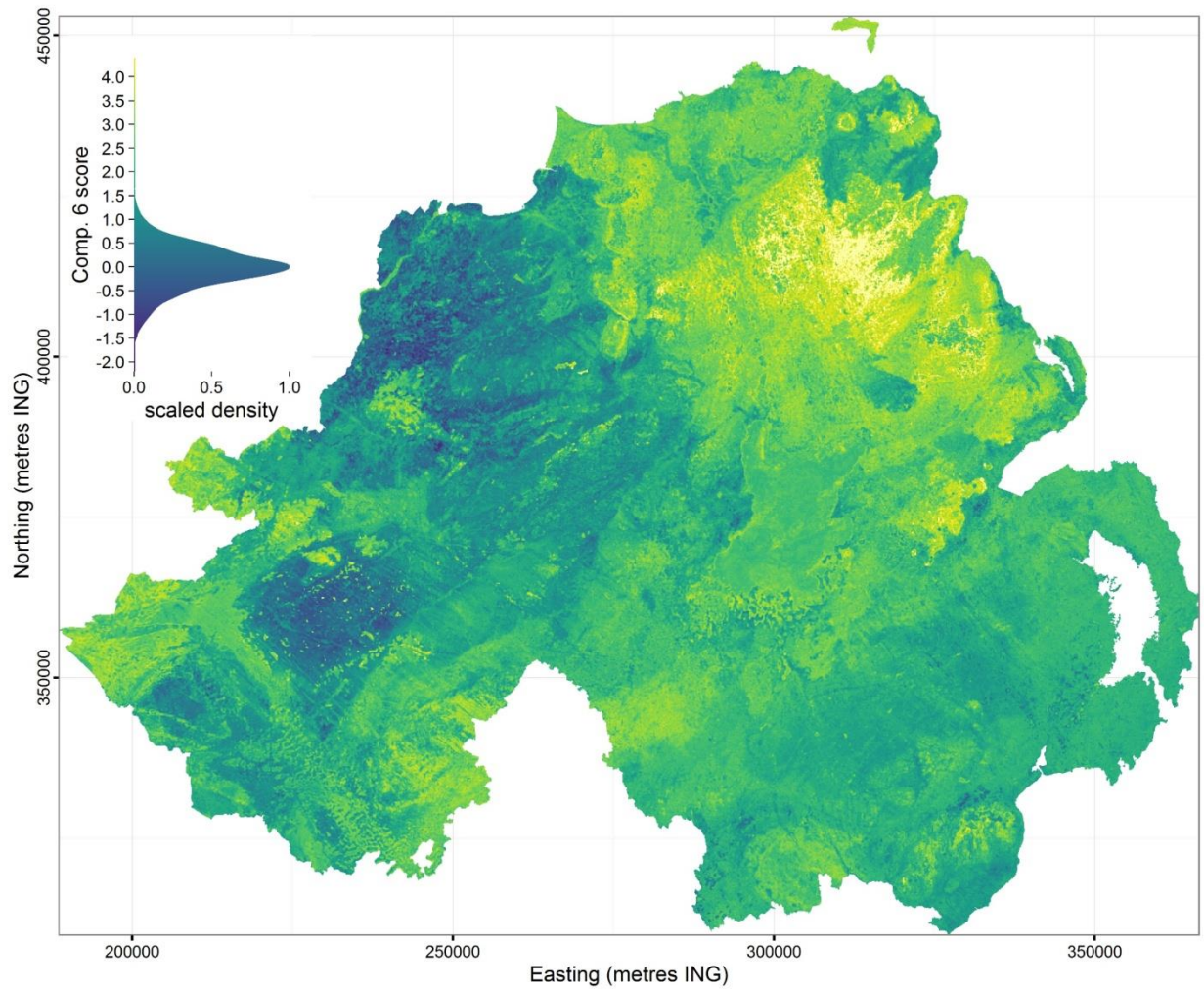


240

241

Fig. 9. Top) Map of independent component 5 of 1lr transformed shallow soil geochemistry, produced using geophysical covariates and the random forest machine learning algorithm. Bottom) Element loadings on independent component 5, as centred log-ratios (relative enrichments/depletions).

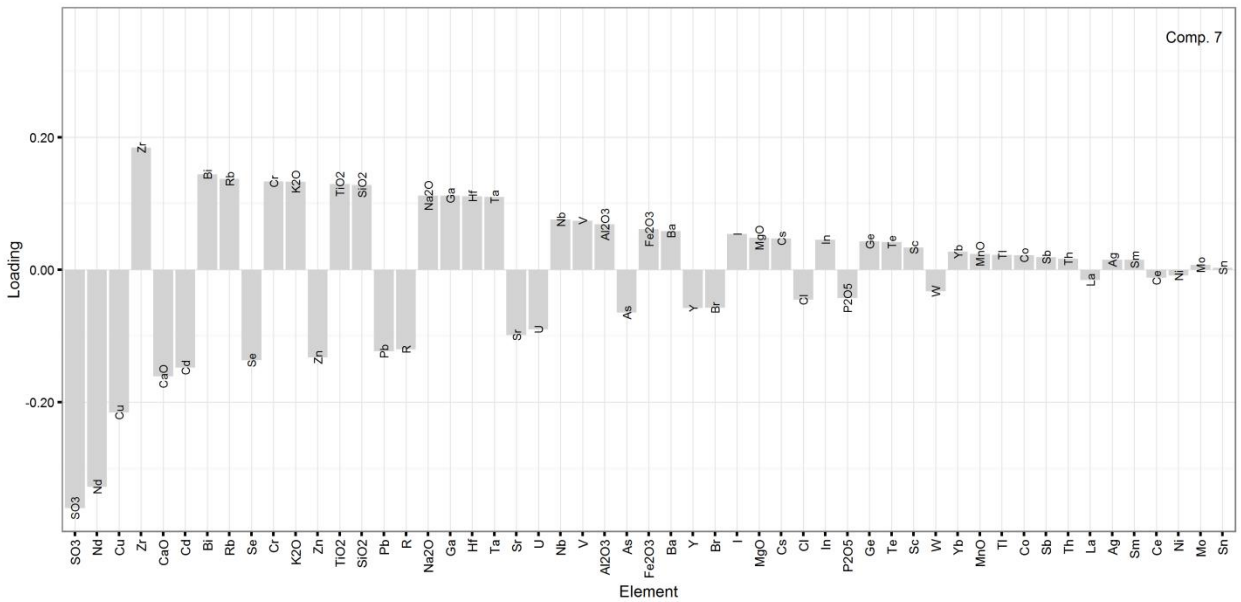
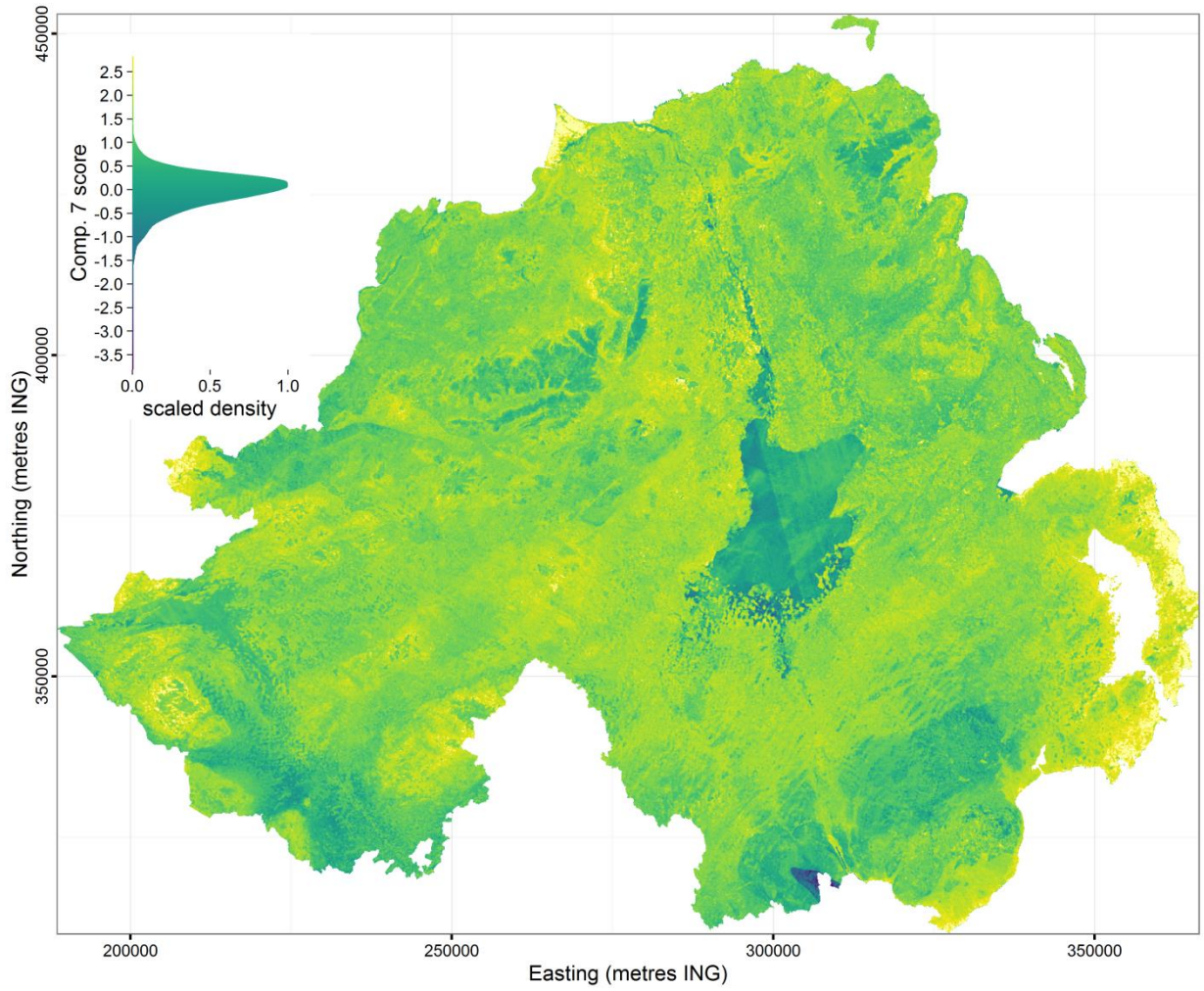
244



245

246 **Fig. 10.** Top) Map of independent component 6 of ilr transformed shallow soil geochemistry, produced using geophysical
 247 covariates and the random forest machine learning algorithm. Bottom) Element loadings on independent component 6, as
 248 centred log-ratios (relative enrichments/depletions).

249



251

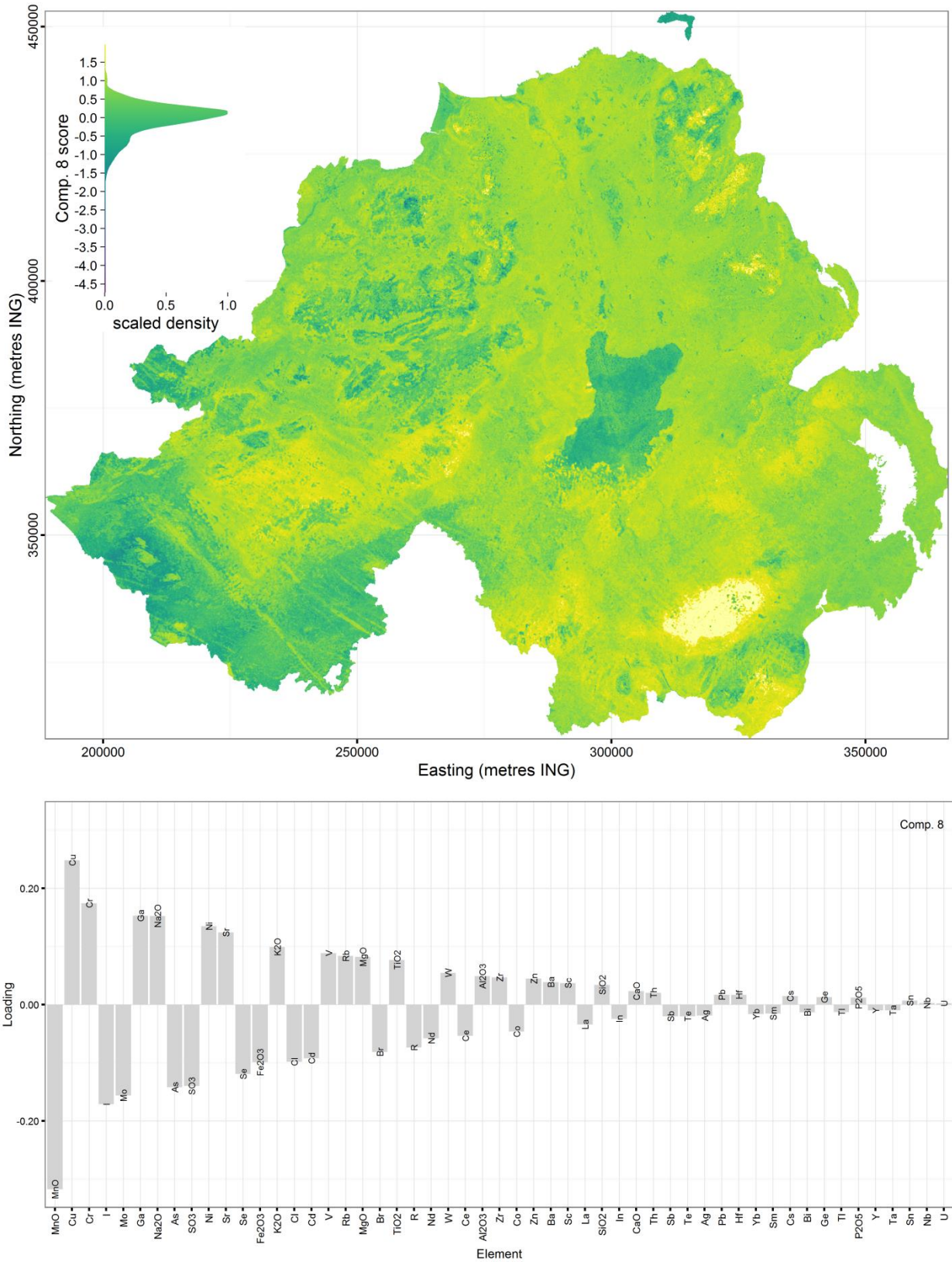
252

Fig. 11. Top) Map of independent component 7 of ilr transformed shallow soil geochemistry, produced using geophysical covariates and the random forest machine learning algorithm. Bottom) Element loadings on independent component 7, as centred log-ratios (relative enrichments/depletions).

253

254

255



257

258

Fig. 12. Top) Map of independent component 8 of ilr transformed shallow soil geochemistry, produced using geophysical covariates and the random forest machine learning algorithm. Bottom) Element loadings on independent component 8, as centred log-ratios (relative enrichments/depletions).

259

260

261

262 **5. Discussion**

263 *5.1 Independent Component 1*

264 Component 1 is the largest component of the chemical composition of Northern Ireland's soils,
265 accounting for 39% of the total variance. The component is positively skewed, with a second mode
266 in the long tail of the data. With background knowledge it is clear from the map (Fig. 5) that this
267 component represents the separation of peat (high values) from all other soils (low values). The
268 Random Forest algorithm has also predicted high values for this component in water bodies, which is
269 likely to be in recognition of the relationship between peat and gamma attenuation due to water
270 content (Beamish, 2013). There are no soil samples within the water bodies and so this is an
271 untestable extrapolation of logic by the Random Forest, but it is likely to hold some truth.

272 In terms of element loadings (Fig. 5), Component 1 represents a depletion of neodymium, gallium,
273 and manganese and an enrichment of chlorine, bromine, sulphur and unmeasured remainder 'R' (a
274 proxy for loss on ignition; Kirkwood et al., 2016a). These loadings confirm the identity of Component
275 1 as a separator of peat from non-peat soils; at high positive scores Component 1 is enriched in
276 volatile elements that often associate with organic material, and depleted in elements which are
277 associated with lithic material i.e. rock forming minerals.

278 *5.2 Independent Component 2*

279 Component 2 accounts for 10.6% of the variance in Northern Ireland's soil composition. As can be
280 seen from the map (Fig. 6), Component 2 is not entirely invariant to peat, and this is captured in the
281 element loadings; with chlorine, sulphur and the unmeasured remainder 'R' the top three
282 enrichments. However, Component 2 has successfully separated the basalts of the early Paleogene
283 Antrim Lava Group (Cooper and Johnston, 2004c) in the north east from surrounding sedimentary
284 rocks. It also captures, with the same negative scores, the dyke swarms in the west (Cooper et al.,
285 2012), indicating their mafic composition (with loadings of nickel, chromium, iron and magnesium).
286 In the south east Component 2 has separated the Late Caledonian Newry Igneous Complex (Cooper

287 and Johnston, 2004a) and Palaeogene Slieve Gullion and Mourne Mountains complexes (Cooper and
288 Johnston, 2004a) from their surrounding Silurian and Ordovician Country rocks (Anderson, 2004).
289 Overall the component seems to have provided power to distinguish between felsic and mafic
290 compositions.

291 *5.3 Independent Component 3*

292 Component 3 accounts for 10.5% of the variance in Northern Ireland's soil composition. Again,
293 Component 3 has been influenced by the peat, with enrichments of bromine, iodine and sulphur.
294 However, where the ground is not covered by peat, Component 3 captures some subtle bedrock
295 variations across the entire region (Fig. 7). In the north east the extent of the Antrim Lava Group is
296 well constrained although there is some blurring of the contact between it and underlying
297 Cretaceous rocks most likely due to down slope movement of basalt talus (scree). Also in this part of
298 Northern Ireland the rhyolitic Tardree Complex (Cooper and Johnston, 2004c) is differentiated from
299 the surrounding Antrim Lava Group and it would appear, based on known outcrop of bedrock, that
300 there has been significant north west transport of material by ice during the Quaternary which is
301 consistent with the findings of previous studies (Dempster et al., 2013).

302 To the south east Component 3 separates the Newry Igneous, Slieve Gullion and Mourne Mountains
303 complexes from their surrounding Silurian and Ordovician country rocks. Whilst in the west clear
304 differences are observed between Proterozoic basement rocks (Cooper and Johnston, 2004b) of the
305 Lough Derg Inlier, Tyrone Central Inlier, Dalradian Supergroup (including the Lack Inlier) and younger
306 Devonian and Carboniferous rocks of this area. In addition, rocks of the predominantly mafic Tyrone
307 Igneous Complex (Cooper et al., 2011; Hollis et al., 2012) are also picked out and share similar
308 character to the similarly mafic Antrim Lava Group to the east. This component picks out faults and
309 dykes in the south west and east of the region. Of all the components, Component 3 may provide
310 the single best 'summary' of Northern Ireland's geology at a glance.

311 *5.4 Independent Component 4*

312 Component 4 accounts for 9.5% of the variance in Northern Ireland's soil composition. The strongest
313 feature on the map (Fig. 8) is the stark lowlighting of the Paleogene granitoid of the Mourne
314 Mountains relative to surrounding rocks, including other granitoids, of the Southern-Uplands-Down-
315 Longford Terrane in the south. For the Mourne Mountains (negative scores on Component 4)
316 compared to the other granitoids, the element loadings (Fig. 8) suggest a lower calcium, higher
317 thorium and higher rubidium composition, with additional enrichments of lead and arsenic.
318 Movement of Mourne granite debris is apparent in superficial deposits including southward and
319 south-easterly transport by glacial processes onto the Mourne Plain, and northward fluvial transport
320 by the Lagan River. On the north coast, blown sand is apparent at Magilligan Point, the Bann
321 Estuary, Portrush Strand and Bushfoot dune complexes.

322 *5.5 Independent Component 5*

323 Component 5 accounts for 5.2% of the variance in Northern Ireland's soil composition. The most
324 striking feature on the map (Fig. 9) is the Newry Igneous Complex relative to surrounding country
325 rocks of the Southern Uplands-Down-Longford Terrane. To the south east on the Mourne Plain, this
326 signal is repeated and may represent the presence of Newry Igneous Complex detritus in the glacial
327 deposits of this area (Fig. 21). Negative scores are observed in peripheral areas of the Antrim Plateau
328 and are related to the presence of Antrim Lava Group basalt at or close to surface, whilst, more
329 positive score in this area are due mainly to the presence of glacial deposits (Geological Survey of
330 Northern Ireland, 1991).

331 The northern part of mostly mafic Tyrone Igneous Complex has negative scores, whilst the positive
332 scores in southern part are associated with bedrock of the Tyrone Central Inlier (Chew et al., 2008)
333 and the Slieve Gullion granite (Hollis et al., 2013) both of which are essentially felsic in composition.
334 Some parts of the southern area have positive scores because of superficial deposits of glaciofluvial
335 sand and gravel (Geological Survey of Northern Ireland, 1991). In the south east of Northern Ireland

336 to the south west of Lough Erne, component 5 successfully differentiates the Carboniferous
337 limestone and shale dominated Meenymore, Glencar Limestone, Dartry Limestone (inc Knockmore
338 Member) and Benbulbin Shale formations (which have negative scores) from the sandstone
339 dominated Glenade Sandstone Formation (Mitchell, 2004).

340 The element loadings (Fig. 9) indicate that the Antrim Lava Group basalts are relatively enriched in
341 nickel, chromium and sulphur, and that the Newry Igneous Complex is more enriched in sodium than
342 the surrounding country rock.

343 *5.6 Independent Component 6*

344 Component 6 accounts for 4.7% of the variance in Northern Ireland's soil composition. The most
345 striking feature on the map (Fig. 10) is the negative scoring Proterozoic Dalradian Supergroup of the
346 Sperrin Mountains and the NE Antrim Inlier compared to the positive scoring basalts of the Antrim
347 Plateau and the low positive scoring of Lower Carboniferous (red bed) sequences in the Rathlin,
348 Newtown Stewart and Omagh Basins (Fig. 24). Devonian and Carboniferous rocks of the Fintona
349 Block are like the Dalradian Supergroup negative scoring. The element loadings (Fig. 10) suggest that
350 the low scoring terranes are depleted in bismuth, copper and nickel, and enriched in rubidium,
351 thorium and neodymium relative to their Carboniferous surroundings. It is an interesting point that a
352 component which captures only 4.7% of the variance in the data may actually provide the most
353 effective separation of terranes from different geological periods. Traditional geological mapping
354 differentiates rocks according to criteria beyond chemical composition, but there is rarely a
355 boundary between established units that is not also captured by some aspect of chemical
356 composition.

357 *5.7 Independent Component 7*

358 Component 7 (Fig. 11) accounts for 3.5% of the variance in Northern Ireland's soil composition. Most
359 notably, Component 7 reveals the low to negative scoring Newry Igneous Complex compared to its
360 surrounding Ordovician-Silurian country rock of the Southern Uplands-Down-Longford terrane.

361 Within the latter, positive scoring north east – southwest trending packages of Moffat Shale Group
362 rocks are apparent on tract boundaries and although they don't match well with the regional scale
363 bedrock map (Geological Survey of Northern Ireland, 1997) they do correspond closely with recently
364 published interpretations of the Tellus electromagnetic imagery (Beamish et al., 2010; Cooper et al.,
365 2016b). Glacial transport of positive scoring Ordovician-Silurian bedrock detritus is also apparent
366 along the north-northwest orientated Camlough and Newry Faults. Similar to Component 5,
367 Component 7 in the southeast of Northern Ireland successfully differentiates Carboniferous
368 sandstone, limestone and shale formations. Some diagonal striations are visible across Lough
369 Neagh, these are artefacts in the geophysical survey data which have become apparent as the
370 random forest algorithm is forced to use such minor subtleties of the data in order to model such
371 minor components as this one.

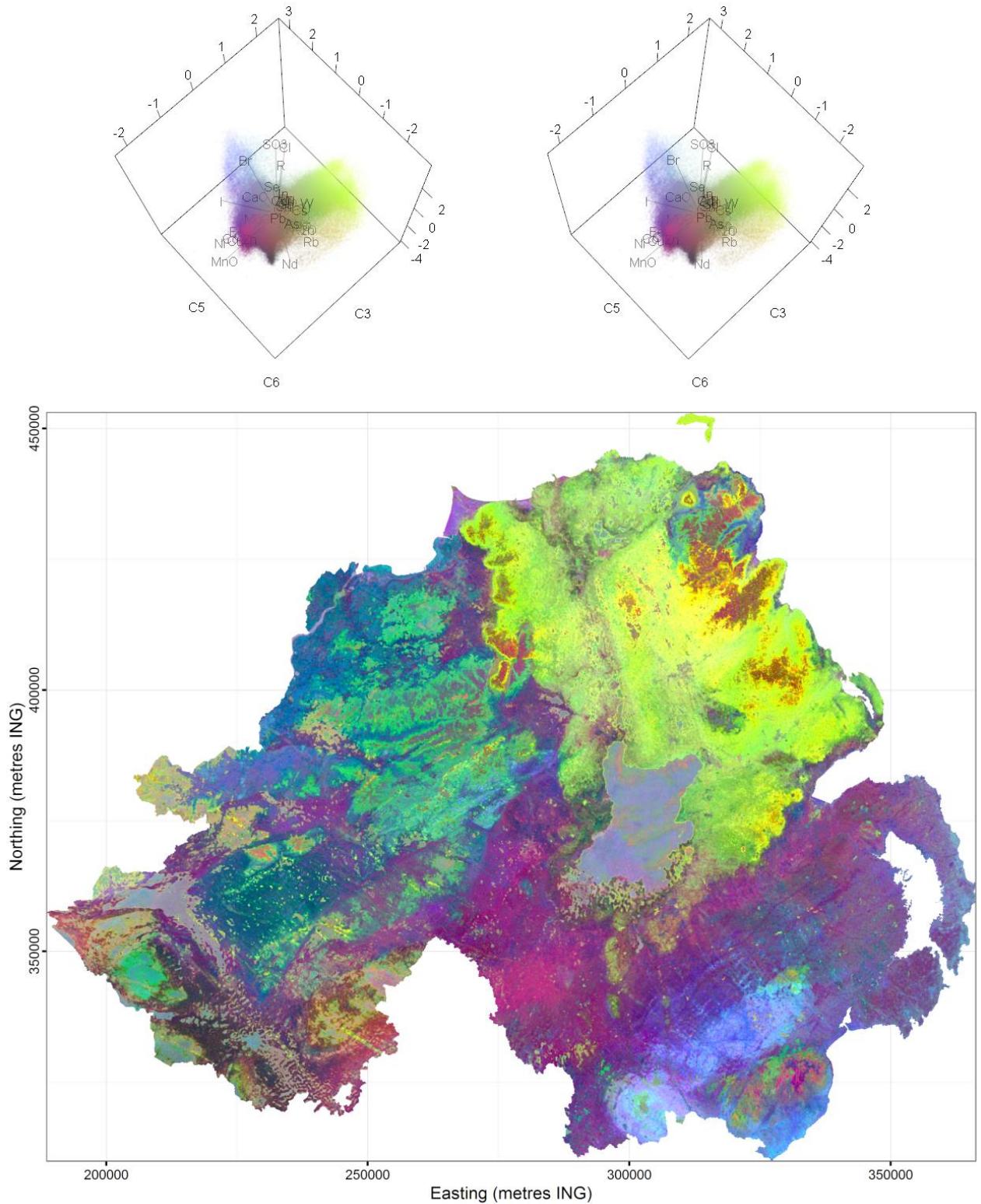
372 The element loadings for Component 7 (Fig. 11) indicate that the central portion of the Newry
373 Igneous Complex is relatively enriched in neodymium, and to a lesser extent copper, zinc and lead. In
374 the terranes of the north west, the loadings would suggest a higher concentration of zirconium,
375 potassium, and silicon in the Carboniferous compared to the Proterozoic.

376 *5.8 Independent Component 8*

377 Component 8 accounts for 2.6% of the variance in Northern Ireland's soil composition, and in terms
378 of element loadings is characterised by relative depletion of manganese and enrichment of copper
379 (Fig. 12). The map of Component 8 (Fig. 12) most notably highlights the positive scoring
380 southwestern part of the Rathfriland Pluton of the Newry Igneous Complex (Cooper et al., 2016a), as
381 well as contrasting between different fault blocks in the sedimentary terrains of the west and
382 highlighting the dykes within them. The central part of the Slieve Gullion Complex is also apparent as
383 a negative scoring area, which corresponds to granophyric rocks (felsic).

384 *5.9 Beyond single components*

385 While separating the geochemical composition of Northern Ireland into constituent independent
386 components provides a solid framework from which to interpret geochemical variations, the best
387 overall impression of Northern Ireland's geochemistry can be obtained by recombining the
388 independent components in ternary colour images (i.e. with a different component representing
389 each of the three channels of human vision; red, green and blue). With only three channels it is not
390 possible to capture all of the geochemical variation at once, but, for whichever three components
391 are chosen, ternary visualisation provides maximal conveyance of information to the viewer. For
392 example, a ternary red-green-blue image of independent components six, three and five (Fig. 13)
393 provides sufficient bedrock detail to reveal all of the features that are present in the geological map
394 (Fig. 1) and more. As the image provides information in a continuous fully-quantitative manner,
395 variation within units can be seen, which is something that a traditional classified map cannot
396 provide, and is likely to be very useful to any geoenvironmental stakeholders.



398

399

400

401

402

403

Fig. 13. Ternary red-green-blue map of independent components six, three and five, each quantile clipped within 0.1 and 99.9%. Above the map, two 3D triplots provide a legend for the meaning of the colours in terms of geochemical composition, this is best viewed in 3D by crossing the eyes. The components were selected for their abilities to differentiate bedrock. The appearance may be psychedelic, but in fact by revealing subtle variations in chemical composition the map captures all the features of the geological map (Fig. 1) and more, all in a fully-quantitative format.

404

405 **6. Conclusion**

406 Compositional FastICA was successful in unmixing the complex geochemistry of Northern Ireland
407 into eight independent and interpretable components, each with distinct elemental loadings to
408 differentiate separate aspects of Northern Ireland's geochemical composition. The use of random
409 forest to map these components on the basis of their relationships with geophysical parameters has
410 provided high-resolution maps of geochemical composition (with all but one more accurate than
411 their IDW interpolated counterparts). By combining these machine learned geochemical component
412 maps into full-colour ternary images, we are presented with a rich visualisation of the geochemical
413 composition of Northern Ireland's soils, with both the chemical resolution of laboratory XRF analysis
414 and the spatial resolution of high-resolution geophysics.

415 By translating geophysical survey data into chemical composition in this way, we are able to capture
416 all of the features of a traditional geological map and more, with the significant benefit that the
417 continuous fully-quantitative format reveals intra-unit variation and is derived from a transparent,
418 reproducible, data-driven workflow. This approach would be particularly useful in reconnaissance
419 mapping of unexplored terrains, as well as in providing quantitative evidence, consistent across the
420 entire region, from which to update and unify legacy maps.

421 **Acknowledgements**

422 This research was funded by the British Geological Survey. The geochemical and airborne
423 geophysical data used in the study come from the Tellus Project which was funded by DETI and by
424 the Building Sustainable Prosperity scheme of the Rural Development Programme (Department of
425 Agriculture and Rural Development of Northern Ireland). Thanks to all colleagues and reviewers who
426 have helped to guide this study.

427

428 References

- 429 Aitchison, J., 1986. The statistical analysis of compositional data. Chapman & Hall, London.
- 430 Anderson, T., 2004. Southern Uplands - Down Longford Terrane, in: Mitchell, W.I. (Ed.), The Geology
431 of Northern Ireland: Our Natural Foundation, Second edition ed. Geological Survey of
432 Northern Ireland, Belfast, pp. 41-60.
- 433 Beamish, D., 2013. Gamma ray attenuation in the soils of Northern Ireland, with special reference to
434 peat. *Journal of environmental radioactivity* 115, 13-27.
- 435 Beamish, D., Kimbell, G., Stone, P., Anderson, T., 2010. Regional conductivity data used to reassess
436 Early Palaeozoic structure in the Northern Ireland sector of the Southern Uplands–Down–
437 Longford terrane. *Journal of the Geological Society* 167, 649-657.
- 438 Beamish, D., Young, M., 2009. Geophysics of Northern Ireland: the Tellus effect. *First Break* 27.
- 439 Breiman, L., 2001. Random forests. *Machine learning* 45, 5-32.
- 440 Carranza, E.J.M., Laborte, A.G., 2015. Random forest predictive modeling of mineral prospectivity
441 with small number of prospects and data with missing values in Abra (Philippines).
442 *Computers & Geosciences* 74, 60-70.
- 443 Chayes, F., 1960. On correlation between variables of constant sum. *Journal of Geophysical research*
444 65, 4185-4193.
- 445 Chew, D., Flowerdew, M., Page, L., Crowley, Q., Daly, J., Cooper, M., Whitehouse, M., 2008. The
446 tectonothermal evolution and provenance of the Tyrone Central Inlier, Ireland: Grampian
447 imbrication of an outboard Laurentian microcontinent? *Journal of the Geological Society*
448 165, 675-685.
- 449 Cooper, M., 2004. The geology of Northern Ireland: our natural foundation, Second edition ed.
450 Geological Survey of Northern Ireland.
- 451 Cooper, M., Anderson, H., Walsh, J., Van Dam, C., Young, M., Earls, G., Walker, A., 2012. Palaeogene
452 Alpine tectonics and Icelandic plume-related magmatism and deformation in Northern
453 Ireland. *Journal of the Geological Society* 169, 29-36.
- 454 Cooper, M., Crowley, Q., Hollis, S., Noble, S., Roberts, S., Chew, D., Earls, G., Herrington, R.,
455 Merriman, R., 2011. Age constraints and geochemistry of the Ordovician Tyrone Igneous
456 Complex, Northern Ireland: implications for the Grampian orogeny. *Journal of the Geological*
457 *Society* 168, 837-850.
- 458 Cooper, M., Johnston, T., 2004a. Palaeogene intrusive igneous rocks, in: Mitchell, W.I. (Ed.), The
459 Geology of Northern Ireland: Our Natural Foundation, Second edition ed. Geological Survey
460 of Northern Ireland, Belfast, pp. 179-198.
- 461 Cooper, M.R., Anderson, P.C.D.J., Stevenson, C.T.E., Ellam, R.M., Meighan, I.G., Crowley, Q.G., 2016a.
462 Shape and intrusion history of the Late Caledonian, Newry Igneous Complex, Northern
463 Ireland, in: Young, M.E. (Ed.), *Unearthed: impacts of the Tellus surveys of the north of*
464 *Ireland*. Royal Irish Academy.
- 465 Cooper, M.R., Floyd, J.D., Barker, G.J., Ture, M.D., Hodgson, J.A., McConnell, B.J., Warke, M.R.,
466 2016b. The geological significance of electrical conductivity anomalies of the Ordovician-
467 Silurian Moffat Shale Group, Northern Ireland., in: Young, M.E. (Ed.), *Unearthed: impacts of*
468 *the Tellus surveys of the north of Ireland*. Royal Irish Academy.
- 469 Cooper, M.R., Johnston, T., 2004b. Central Highlands (Grampian) Terrane - Metamorphic Basement,
470 in: Mitchell, W.I. (Ed.), *The Geology of Northern Ireland: Our Natural Foundation*, Second
471 edition ed. Geological Survey of Northern Ireland, Belfast, pp. 9-24.
- 472 Cooper, M.R., Johnston, T., 2004c. Palaeogene extrusive igneous rocks, in: Mitchell, W.I. (Ed.), *The*
473 *Geology of Northern Ireland: Our Natural Foundation*, Second edition ed. Geological Survey
474 of Northern Ireland, Belfast, pp. 167-178.
- 475 Cracknell, M., Reading, A., McNeill, A., 2014. Mapping geology and volcanic-hosted massive sulfide
476 alteration in the Hellyer–Mt Charter region, Tasmania, using Random Forests™ and Self-
477 Organising Maps. *Australian Journal of Earth Sciences* 61, 287-304.

478 Cracknell, M.J., Reading, A.M., 2014. Geological mapping using remote sensing data: A comparison
479 of five machine learning algorithms, their response to variations in the spatial distribution of
480 training data and the use of explicit spatial information. *Computers & Geosciences* 63, 22-33.

481 Darnley, A.G., 1990. International geochemical mapping: a new global project. *Journal of*
482 *Geochemical Exploration* 39, 1-13.

483 Delorme, A., Makeig, S., 2004. EEGLAB: an open source toolbox for analysis of single-trial EEG
484 dynamics including independent component analysis. *Journal of neuroscience methods* 134,
485 9-21.

486 Dempster, M., Dunlop, P., Scheib, A., Cooper, M., 2013. Principal component analysis of the
487 geochemistry of soil developed on till in Northern Ireland. *Journal of Maps* 9, 373-389.

488 Egozcue, J.J., Pawlowsky-Glahn, V., Mateu-Figueras, G., Barcelo-Vidal, C., 2003. Isometric logratio
489 transformations for compositional data analysis. *Mathematical Geology* 35, 279-300.

490 Evans, J.S., Murphy, M.A., Holden, Z.A., Cushman, S.A., 2011. Modeling species distribution and
491 change using random forest, *Predictive Species and Habitat Modeling in Landscape Ecology*.
492 Springer, pp. 139-159.

493 Filzmoser, P., Hron, K., Reimann, C., 2009a. Principal component analysis for compositional data with
494 outliers. *Environmetrics* 20, 621-632.

495 Filzmoser, P., Hron, K., Reimann, C., Garrett, R., 2009b. Robust factor analysis for compositional data.
496 *Computers & Geosciences* 35, 1854-1861.

497 Garnier, S., 2015. viridis: Matplotlib Default Color Map. R package version 0.2.

498 Geological Survey of Northern Ireland, G., 1991. Geological Map of Northern Ireland (Quaternary).
499 Geological Survey of Northern Ireland, Belfast.

500 Geological Survey of Northern Ireland, G., 1997. Geological Map of Northern Ireland (Solid).
501 Geological Survey of Northern Ireland, Belfast.

502 Gislason, P.O., Benediktsson, J.A., Sveinsson, J.R., 2006. Random forests for land cover classification.
503 *Pattern Recognition Letters* 27, 294-300.

504 Grunsky, E.C., Drew, L.J., Sutphin, D.M., 2009. Process recognition in multi-element soil and stream-
505 sediment geochemical data. *Applied Geochemistry* 24, 1602-1616.

506 Harris, J., Grunsky, E., Behnia, P., Corrigan, D., 2015. Data-and knowledge-driven mineral
507 prospectivity maps for Canada's North. *Ore Geology Reviews*.

508 Henderson, B.L., Bui, E.N., Moran, C.J., Simon, D., 2005. Australia-wide predictions of soil properties
509 using decision trees. *Geoderma* 124, 383-398.

510 Hinze, W.J., Von Frese, R.R., Saad, A.H., 2013. Gravity and magnetic exploration: Principles, practices,
511 and applications. Cambridge University Press.

512 Hodgson, J., Young, M., 2016. The Tellus airborne geophysical data and results, in: Young, M. (Ed.),
513 *Unearthed: impacts of the Tellus surveys of the north of Ireland*. Royal Irish Academy,
514 Dublin.

515 Hollis, S.P., Cooper, M.R., Roberts, S., Earls, G., Herrington, R., Condon, D.J., 2013. Stratigraphic,
516 geochemical and U–Pb zircon constraints from Slieve Gallion, Northern Ireland: a correlation
517 of the Irish Caledonian arcs. *Journal of the Geological Society* 170, 737-752.

518 Hollis, S.P., Roberts, S., Cooper, M.R., Earls, G., Herrington, R., Condon, D.J., Cooper, M.J., Archibald,
519 S.M., Piercey, S.J., 2012. Episodic arc-ophiolite emplacement and the growth of continental
520 margins: Late accretion in the Northern Irish sector of the Grampian-Taconic orogeny.
521 *Geological Society of America Bulletin* 124, 1702-1723.

522 Hyvarinen, A., 1999. Fast and robust fixed-point algorithms for independent component analysis.
523 *IEEE transactions on Neural Networks* 10, 626-634.

524 Hyvärinen, A., Oja, E., 2000. Independent component analysis: algorithms and applications. *Neural*
525 *networks* 13, 411-430.

526 Johnson, C., Breward, N., Ander, E., Ault, L., 2005. G-BASE: baseline geochemical mapping of Great
527 Britain and Northern Ireland. *Geochemistry: Exploration, Environment, Analysis* 5, 347-357.

528 Kirkwood, C., Cave, M., Beamish, D., Grebby, S., Ferreira, A., 2016a. A machine learning approach to
529 geochemical mapping. *Journal of Geochemical Exploration* 167, 49-61.

530 Kirkwood, C., Everett, P., Ferreira, A., Lister, B., 2016b. Stream sediment geochemistry as a tool for
531 enhancing geological understanding: An overview of new data from south west England.
532 *Journal of Geochemical Exploration* 163, 28-40.

533 Lawrence, R.L., Wood, S.D., Sheley, R.L., 2006. Mapping invasive plants using hyperspectral imagery
534 and Breiman Cutler classifications (RandomForest). *Remote Sensing of Environment* 100,
535 356-362.

536 Liu, B., Guo, S., Wei, Y., Zhan, Z., 2014. A Fast Independent Component Analysis Algorithm for
537 Geochemical Anomaly Detection and Its Application to Soil Geochemistry Data Processing.
538 *Journal of Applied Mathematics* 2014.

539 Makeig, S., Bell, A.J., Jung, T.-P., Sejnowski, T.J., 1996. Independent component analysis of
540 electroencephalographic data. *Advances in neural information processing systems*, 145-151.

541 McKinley, J.M., Hron, K., Grunsky, E.C., Reimann, C., de Caritat, P., Filzmoser, P., van den Boogaart,
542 K.G., Tolosana-Delgado, R., 2016. The single component geochemical map: Fact or fiction?
543 *Journal of Geochemical Exploration* 162, 16-28.

544 Mitchell, W.I., 2004. Carboniferous, in: Mitchell, W.I. (Ed.), *The Geology of Northern Ireland: Our
545 Natural Foundation*, Second edition ed. Geological Survey of Northern Ireland, Belfast, pp.
546 79-116.

547 Pawlowsky-Glahn, V., Egozcue, J., 2006. Compositional data and their analysis: an introduction.
548 Geological Society, London, Special Publications 264, 1-10.

549 Pawlowsky-Glahn, V., Egozcue, J.J., Tolosana Delgado, R., 2007. Lecture notes on compositional data
550 analysis.

551 Pearson, K., 1896. Mathematical Contributions to the Theory of Evolution. --On a Form of Spurious
552 Correlation Which May Arise When Indices Are Used in the Measurement of Organs.
553 *Proceedings of the royal society of london* 60, 489-498.

554 R Core Team, 2016. R: A Language and Environment for Statistical Computing. R Foundation for
555 Statistical Computing, Vienna, Austria.

556 Rodriguez-Galiano, V., Sanchez-Castillo, M., Chica-Olmo, M., Chica-Rivas, M., 2015. Machine learning
557 predictive models for mineral prospectivity: An evaluation of neural networks, random
558 forest, regression trees and support vector machines. *Ore Geology Reviews*.

559 Rodriguez-Galiano, V.F., Ghimire, B., Rogan, J., Chica-Olmo, M., Rigol-Sanchez, J.P., 2012. An
560 assessment of the effectiveness of a random forest classifier for land-cover classification.
561 *ISPRS Journal of Photogrammetry and Remote Sensing* 67, 93-104.

562 Seligman, M., 2016. Rborist: Extensible, Parallelizable Implementation of the Random Forest, R
563 package version 0.1-1 ed.

564 Wiesmeier, M., Barthold, F., Blank, B., Kögel-Knabner, I., 2011. Digital mapping of soil organic matter
565 stocks using Random Forest modeling in a semi-arid steppe ecosystem. *Plant and soil* 340, 7-
566 24.

567 Yang, J., Cheng, Q., 2015. A comparative study of independent component analysis with principal
568 component analysis in geological objects identification, Part I: Simulations. *Journal of
569 Geochemical Exploration* 149, 127-135.

570 Young, M., Donald, A., 2013. A guide to the Tellus data. Geological Survey of Northern Ireland,
571 Belfast.

572